European Scientific Journal July 2016 /SPECIAL/ edition ISSN: 1857 – 7881 (Print) e - ISSN 1857- 7431

Heat Transfer Investigation Of Aluminum Oxide Nanofluids In Heat Exchangers

Roy Jean Issa, Ph.D.
West Texas A&M University, USA

Abstract

An experimental study was conducted to investigate the use of water-based aluminum oxide nanofluids in enhancing the heat transfer performance of heat exchangers. Two types of heat exchangers were studied: a block-type heat exchanger for an electronic system cooling, and a radiator-type heat exchanger simulating an automobile cooling system. Tests conducted on the block heat exchanger used 20 nm alumina particles at a concentration of 5% by mass (1.3% by volume), while tests conducted on the radiator-type heat exchanger used 50 nm alumina particles at a concentration of 3% by mass (0.8% by volume). Tests conducted on the electronic heat sink system show an average enhancement of about 20% in heat transfer coefficient, while tests conducted on the radiator-type heat exchanger show a substantial enhancement in heat exchanger effectiveness that reaches almost 49%. Results demonstrate that the application of nanofluids in low concentrations is sufficient to cause a considerable improvement in the system‘s thermal performance. Results also show that the increase in bulk flow heat transfer coefficient happens at the expense of the increase in fluid pumping power caused by the increase in fluid viscosity.

Keywords: Heat Transfer Coefficient, Effectiveness, Nanofluid, AL_2O_3

Introduction

With the ever increasing demand for cooling power in heat exchangers, huge efforts have been devoted to their heat transfer enhancement. Research conducted during the last few years have shown significant improvements in the thermal properties of conventional heat transfer fluids by the addition of nanoparticles to the base fluids. Tests conducted on water-based AL_2O_3 nanofluids have shown enhancement in thermal conductivity that varied from a modest 1.4% at 0.3% volume concentration with 30 nm particles (Lee, 2008), to 10% at 3% volume concentration with 43 nm particles (Chandrasekar, 2010), to 24% at 4% volume concentration with 33 nm particles (Eastman, 1997), to 30% at 18%

volume concentration with 36 nm particles (Mintsa, 2009), and to a considerable enhancement of 88% at 12% volume concentration with 75 nm particles (Ghanbarpour, 2014). It is clearly evident in those studies that the bulk fluid thermal conductivity in general increases with the increase in nanoparticles volume concentration.

The benefit of using nanofluids in heat exchanger applications have been investigated by several researchers. In the cooling of a microchannel heat sink, Ijam et al. (2012) has shown that adding Al_2O_3 nanoparticles to water at 4% volume concentration improved the heat flux by about 3 %, and by about 17.3% when the particle volume concentration was 0.8%. Ijam and Saidur (2012) also showed that the addition of SiC nanoparticles to water at 4% volume fraction resulted in an improvement between 7.3 to 12.4% in heat flux. Selvakumar and Suresh (2012) studied the performance of CuO water-based nanofluid in an electronic heat sink. Their study revealed a 29% improvement in heat transfer coefficient for 0.2% volume fraction of CuO in deionized water. Hashemi et al. (2012) studied heat transfer enhancement in a nanofluid-cooled miniature heat sink application. Their study showed an enhancement in the heat transfer coefficient by about 27% when using SiO_2 at a concentration of 5% concentration by volume. Khedkar et al. (2013) studied the heat transfer in a concentric tube heat exchanger with different volume fractions of water-based Al_2O_3 nanofluids. It was observed that at 3% volume fraction, the optimal overall heat transfer coefficient was about 16% higher than water. Sun et al. (2015) analyzed the flow and convective heat transfer characteristics of Fe_2O_3 water-based nanofluids inside inner grooved copper and smooth cooper tubes. For the same mass fraction of Fe_2O_3 nanoparticles, the convective heat transfer coefficient was better in the inner grooved copper tube than in the smooth copper tube. The enhancement in heat transfer coefficient associated with the inner grooved copper tube was about 33.5% for Fe_2O_3 mass concentration of 0.4%. All of the above researchers have examined the effect of nanoparticles concentration on heat transfer enhancement, and have studied different types of nanoparticles. However, there are contradictory conclusions on the heat transfer enhancement at lower nanoparticle concentrations among different researchers. Also, still limited research studies have been conducted on the evaluation of alumina nanofluid properties and their performance in heat exchanger applications. The current study aims at investigating some of these issues in addition to investigating the thermal and rheological properties of water-based alumina nanofluids.

Experimental Setup:

a) Electronic Heat Sink Application

A closed-loop cooling system using block heat exchangers was built to evaluate the heat transfer performance associated with the use of a water-based nanofluid with alumina particles as a cooling fluid. A general picture of the experimental setup is shown in figure 1a. The nanofluid was prepared by mixing alumina nanoparticles with 20 nm average size in deionized water for a suspension concentration of 5% by mass (1.3% by volume). A digital geared-pump was used to pressurize the nanofluid for circulation in the closed-loop system. Two block heat exchangers were used in the system: one to heat the nanofluid (HXR1), and the other to cool the fluid (HXR2). The interior of the block heat exchanger (figure 1b) consisted of 10 channels through which the cooling fluid travelled back and forth.

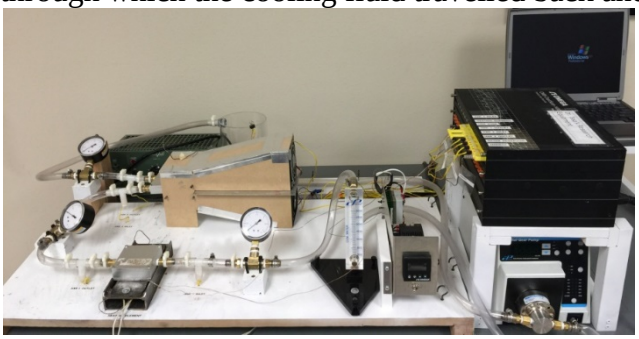

Figure 1a. Experimental setup of the electronic heat sink system.

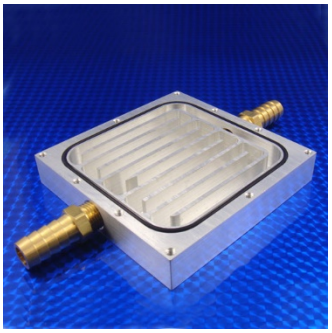

Figure 1b. Block heat exchanger.

The heat exchanger that was used to heat the nanofluid sat on top of a 500 W plate heater separated by a 6.2 mm thick aluminium plate. A temperature control system was used to control the input heat to the base plate of the heat exchanger. The heat exchanger that was used for cooling the nanofluid sat approximately five inches above the base of the closed-loop system. Two cooling fans rated at 120 cfm each were used to cool the upper and lower surfaces of this heat exchanger. Once the fluid exited HXR2 it flowed into a 2-litres reservoir tank. A compact digital mixer system providing a top speed of 2,500 rpm was embedded in the tank. To achieve closed-loop circulation, the outlet from the reservoir tank fed directly into the pump inlet. Thermocouples were embedded at various locations to record the temperature variation throughout the system.

b) Radiator-Type Heat Exchanger Application

Another closed-loop cooling system was also constructed to evaluate the performance of a radiator-type heat exchanger as shown in the sketch of figure 2. The heat exchanger (202 mm x 89 mm x 160 mm) had a 10-pass

cross-flow finned-tubes with a single tube inlet and outlet, where the tubes were arranged in a staggered array. Each tube had an inner diameter of 7.73 mm, an outer diameter of 9.5 mm, and a length of 12.7 cm. 80 fin plates of 0.15 mm thickness, 120 mm width, and 38 mm depth were packaged normal to the tubes to form narrow passes having 1.4 mm separation distance where air blowing from a fan passed through. A collection tank with a high-speed agitator thoroughly mixed the nanofluid, alumina-water based using 50 nm AL_2O_3 particles with a mass concentration of 3% (0.8% by volume), before it was circulated using a circulation pump. A controlled heating system was installed in the tank to maintain the circulating fluid temperature within a desired range. The fluid was cooled using a blowing fan that was attached on one side of the heat exchanger. Thermocouples and flow sensors were installed throughout the system to monitor the fluids temperature and pressure, and were connected to a data acquisition device to record the data.

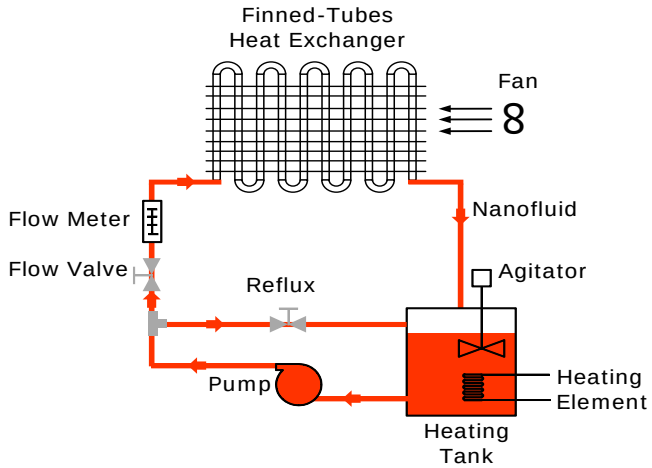

Figure 2. Experimental setup of the radiator-type heat exchanger system.

Property Measurements

Nanofluid test samples using 20 and 50 nm AL_2O_3 particles in distilled water of various concentrations were prepared and tested in a laboratory experimental setup for the determination of thermal conductivity. Thermal conductivity was measured using a KD2 Pro thermal properties analyzer by Decagon Devices. Details about the design and working of the KD2 Pro device can be found in the operator's manual (Decagon Devices, 2010). The analyser consists of a microcontroller with several needle sensors that can be used. KS-1 sensor needle was selected to determine the thermal conductivity of the nanofluids. The needle contains both a heating element and a thermistor. The needle, 1.3 mm in diameter and 6 cm long, was inserted vertically (to minimize natural convection) inside a test tube

containing the nanofluid sample (figure 3). Tests were carried out at a temperature close to 46 ^{o}C, and for nanoparticles mass concentration of up to 40%. Tests reveal that the thermal conductivity of the nanofluid increases with the mass fraction (figure 4). However, there is a slight difference in thermal conductivity between the 20 and 50 nm particle suspensions.

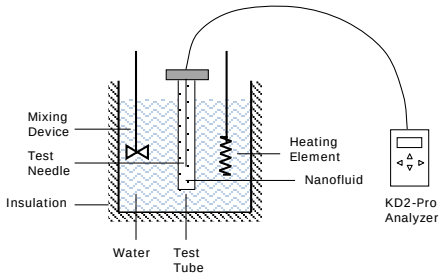

Figure 3. Experimental setup for thermal conductivity analysis.

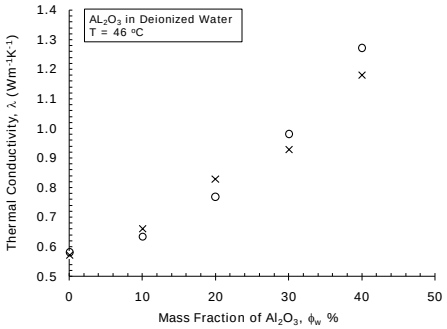

Figure 4. Thermal conductivity versus alumina mass concentration.

Rheological tests were conducted on the same samples originally used for thermal property evaluation. Rheological properties were conducted using UL adapter attached to LVDVII+Pro viscometer. Suspensions were mixed thoroughly using a high-speed mixing device for about 30 minutes before the viscosity tests were carried out. All tests were performed at a temperature ranging from 45 to 49 ^{o}C. Figures 5 and 6 show the variation in the nanofluid viscosity for 20 and 50 nm alumina particles, respectively as function of the shear rate and nanoparticles concentration. Suspensions with 50 nm particles show an increase in viscosity with the increase in shear rate; thus, a shear thickening fluid behaviour (dilatant fluid). However, suspensions with 20 nm particles show a decrease in viscosity with the increase in shear rate for the nanofluid having 5% mass concentration (i.e., shear thinning fluid), but an increase in viscosity for the nanofluid having 2.5% mass concentration (i.e., shear thickening fluid).

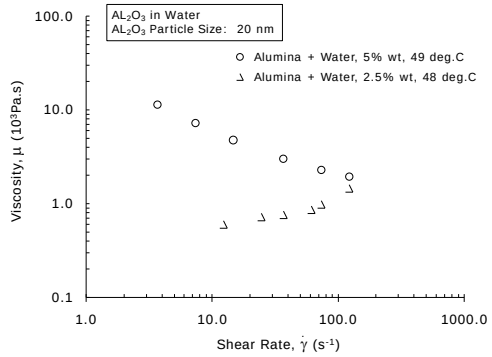

Figure 5. Viscosity versus shear rate for 20 nm alumina-in-water particles.

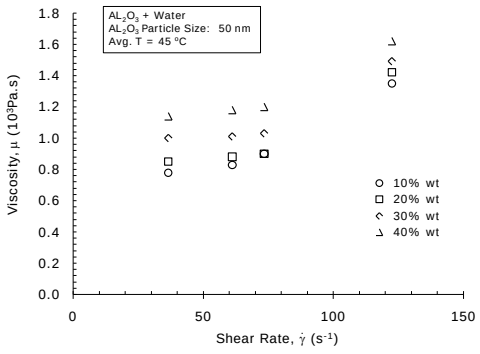

Figure 6. Viscosity versus shear rate for 50 nm alumina-in-water particles.

Heat Transfer Measurements:

a) Electronic Heat Sink Application

Heat transfer tests were carried out on the electronic heat sink system using deionized water-based alumina nanofluid coolant with a 20 nm particles and a mass concentration of 5%. The results were compared to that of a cooling fluid consisting of deionized water. The plate heater was set to a constant temperature of 91 ^{o}C, and the coolant flow rate was varied between 7.8 and 16.1 cm^3s^{-1}. Interface temperatures, and heat exchangers inlet and outlet temperatures were recorded once steady state temperature in the system was reached. The steady state temperature of the coolant associated with the different flow rates ranged from about 47 to 57 ^{o}C. The total volume of the coolant in the system was 2 litres. To minimize the precipitation of nanoparticles in time, a stirring device embedded in the reservoir tank was turned on for the duration of the tests. The heat flux supplied by the electric heater at the base plate of HXR1, q'', is determined from the temperature variation, ΔT, across the plate wall thickness:

$$q'' = \frac{q}{A} = \lambda_p \frac{\Delta T}{\Delta x} \qquad (1)$$

where λ_p is the thermal conductivity of the plate, Δx is the plate thickness, and A is the surface area. The heat transfer coefficient associated with the coolant in the heat exchanger, h_c, is calculated as:

$$h_c = \frac{q''}{T_i - T_f} \qquad (2)$$

where T_i is the heat exchanger base plate interface temperature (interface between the heat exchanger bottom surface and the base plate top surface), and T_f is the bulk mean temperature of the cooling fluid in HXR1. The pumping power of the bulk fluid, P_{power}, is calculated as:

$$P_{power} = \dot{V}\Delta P \qquad (3)$$

Figures 7 and 8 show the wall heat flux (at the base of HXR1) and the coolant heat transfer coefficient as function of the bulk mass flow rate for the case of water-based alumina nanofluid and deionized water, respectively. The wall heat flux and coolant heat transfer coefficient are shown to increase with the increase in bulk mass flow rate. Comparison between figures 7 and 8, show water-based alumina nanofluid has higher values for both the wall heat flux and heat transfer coefficient. An average increase by about 24% is seen in the wall heat flux for the case of water-based nanofluid compared to the case of deionized water. The heat transfer coefficient is also shown to increase by about 20% for the case of water-based nanofluid.

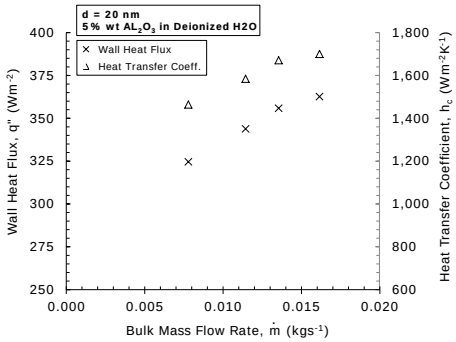

Figure 7. Wall heat flux versus mass flow rate (5% wt AL_2O_3).

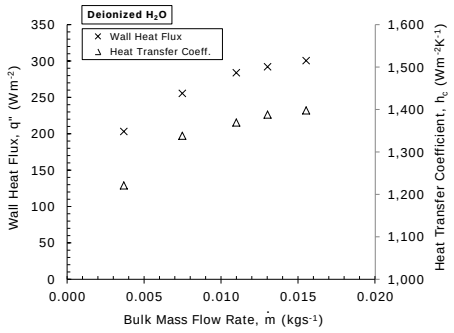

Figure 8. Wall heat flux versus mass flow rate (Deionized water).

Figure 9 shows the decrease in the heated wall cross-section temperature (at the base of HXR1) as function of bulk mass flow rate. For the considered flow rates, the decrease in temperature ranged from 23.7 to 25.8 ^oC for the nanofluid test case, while it ranged from 18.8 to 21.7 ^oC for the deionized water test case. Figure 9 clearly shows an additional temperature drop (i.e., enhancement) between 4.1 and 4.9 ^oC when alumina nanofluid instead of deionized water is used as a coolant.

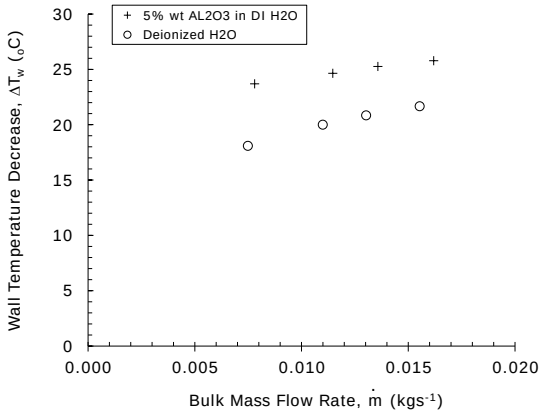

Figure 9. Decrease in wall temperature versus bulk mass flow rate.

Figure 10 shows the pressure drop across HXR1 heat exchanger as function of the bulk mass flow rate. The pressure drop is shown to increase with mass flow rate and with the addition of nanoparticles to the base fluid. The relationship between bulk fluid heat transfer coefficient and pumping power is shown in figure 11. The increase in heat transfer coefficient is shown to occur at the expense of pumping power increase. But for the same pumping power, the presence of nanoparticles in the base fluid is shown to have a significant effect on the increase in heat transfer coefficient, and therefore cooling efficiency.

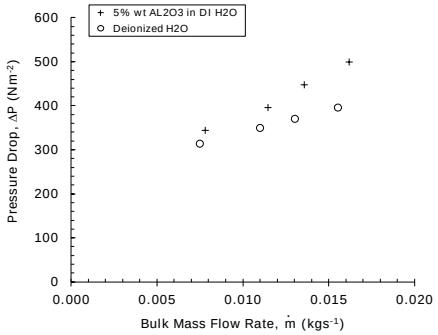

Figure 10. Pressure drop versus bulk mass flow rate.

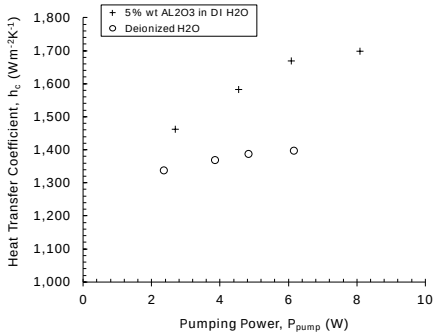

Figure 11. Heat transfer coefficient versus pump power.

b) Radiator-Type Heat Exchanger Application

Heat transfer tests were also performed on the radiator-type heat exchanger. In this case, the water-based alumina nanofluid consisted of 50 nm alumina particles suspensions having a mass concentration of 3%. The performance of the heat exchanger using the nanofluid as a circulating fluid was also compared to that using distilled water. Several test cases were conducted where the tank immersed heater was set to different temperature settings ranging from 200 to 500 ^{o}C. Temperature data were recorded for about 45 minutes after the system reached steady state condition. Figure 12 shows typical results for the temperature drop between the radiator inlet and outlet for the two types of circulating fluids. As expected, the temperature drop increases with the decrease in volumetric flow rate, and the nanofluid is shown to outperform distilled water.

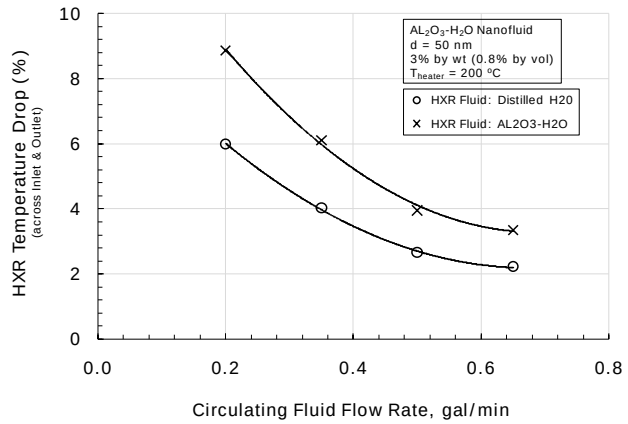

Figure 12. Comparison in radiator temperature drop using aluminum oxide nanofluid versus distilled water.

The radiator heat transfer effectiveness, ε, defined as the ratio of the actual heat transfer, q, to the maximum possible heat transfer that can be achieved, $q_{\max}$, is calculated as follows:

$$\varepsilon = \frac{q}{q_{\max}} = \frac{\dot{m}_f c_{p,f}\left(T_{i,f} - T_{e,f}\right)}{C_{\min}\left(T_{i,f} - T_{i,a}\right)} \qquad (4)$$

where $\dot{m}_f$ is the mass flow rate of the circulating fluid, and $c_{p,f}$ is its specific heat. $C_{\min}$ is the minimum of $\dot{m}_f c_{p,f}$ and $\dot{m}_a c_{p,a}$ where index a indicates air. $T_{i,f}$ and $T_{e,f}$ are the inlet and exit temperatures of the circulating fluid, and $T_{i,a}$ is the air temperature at the fan inlet. Figure 13 shows a comparison in the radiator heat transfer effectiveness between aluminum-oxide water based nanofluid and distilled water. The operating conditions were the same for both fluids. All test cases conducted using the nanofluid showed an increase in heat transfer effectiveness. A substantial enhancement of up to 49% was achieved.

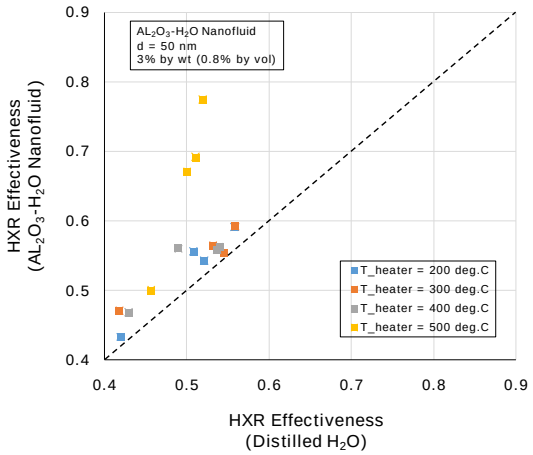

Figure 13. Comparison in radiator heat transfer effectiveness using aluminum oxide nanofluid versus distilled water.

The radiator overall heat transfer coefficient, U, is calculated using the experimental prediction of the heat exchanger log mean temperature difference, ΔT_{LM}:

$$U = \frac{\dot{m}_f c_{p,f}\left(T_{i,f} - T_{e,f}\right)}{A\Delta T_{LM}} \qquad (5)$$

where A is the peripheral area of the radiator tubes. Figure 14 shows a comparison in the radiator overall heat transfer coefficient between the aluminum-oxide nanofluid and distilled water. The conditions are shown for

an average circulating fluid temperature of 40 ^{o}C. An increase of up to 38% can be seen in the highest volumetric flow rate cases.

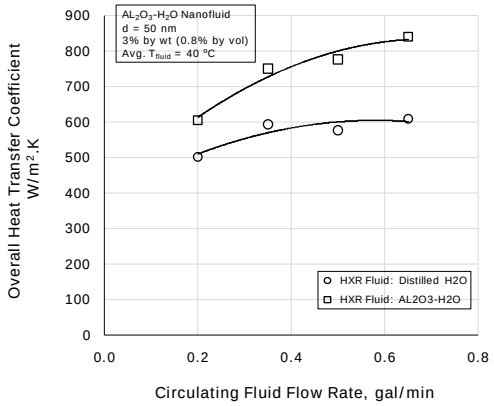

Figure 14. Comparison in radiator overall heat transfer coefficient using aluminum oxide nanofluid versus distilled water.

Conclusion

An experimental study was conducted to investigate the heat transfer performance of two types of heat exchangers using an alumina-water based nanofluid as a circulating fluid: a block-type heat exchanger for an electronic system cooling, and a radiator-type heat exchanger simulating an automobile cooling system. Tests carried out on the block heat exchanger used 20 nm alumina particles at a concentration of 5% by mass, while tests carried out on the radiator-type heat exchanger used 50 nm alumina particles at a concentration of 3% by mass. In both cases, the suspended particles were thoroughly mixed using a high speed agitator before the start of each test. Thermal conductivity tests conducted on the alumina nanofluids show an enhancement of less than 4% for the above mentioned particles concentration levels. Results also show that the increase in bulk flow heat transfer coefficient happens at the expense of the increase in the bulk fluid pumping power due to the increase in bulk fluid viscosity.

Tests on the electronic heat sink system show an average enhancement of about 20% in heat transfer coefficient and 24% in the wall heat flux. Results also show an additional decrease in the heated wall cross-section temperature ranging from 4.1 to 4.9 ^{o}C. Tests conducted on the radiator-type heat exchanger also show a substantial enhancement in heat exchanger effectiveness that reaches almost 49%. Based on these results, it seems that the 4% increase in bulk fluid thermal conductivity may not have been the only driving force behind this substantial increase in the systems heat transfer performance. It is likely possible that another effect such as the Brownian motion of the nanoparticles may have been behind this increase. Since the presence of nanoparticles in the bulk fluid can reduce the thermal

boundary layer thickness (thus enhancing the bulk fluid heat transfer capability), it is possible that the size of the nanoparticles may influence this phenomenon. Even though higher heat transfer performance is achieved in the radiator-type heat exchanger with 50 nm AL_2O_3 particles, the size of the nanoparticles in the base fluid needs to be explored further to verify this effect.

References:

Lee, J. H., Hwang, K. S., Jang, S. P., Lee, B. H., Kim, J. H., Choi, S. U. S., & Choi, C. J. (2008). Effective viscosities and thermal conductivities of aqueous nanofluids containing low volume concentrations of AL_2O_3 nanoparticles *International Journal of Heat and Mass Transfer*, 51, 2651-2656.

Chandrasekar, M., Suresh, S., & Bose, A. C. (2010). Experimental investigations and theoretical determination of thermal conductivity and viscosity of AL_2O_3/water nanofluid. *Experimental Thermal and Fluid Science*, 34, 210-216.

Eastman, J. A., Choi, U. S., Li, S., Thompson, L. J., & Lee, S. (1997). Enhanced thermal conductivity through the development of nanofluids. *Materials Research Society Symposium Proceedings*, 457, 3-11.

Mintsa, H. A., Roy, G., Nguyen, C. T., & Doucet, D. (2009). New temperature dependent thermal conductivity data for water-based nanofluids. *International Journal of Thermal Sciences,* 48, 363-371.

Ghanbarpour, M., Haghigi, E. B., & Khodabandeh, R. (2014). Thermal properties and rheological behaviour of water based AL_2O_3 nanofluid as a heat transfer fluid. *Experimental Thermal and Fluid Science*, 53, 227-235.

Ijam, A., Saidur, R., & Ganesan, P. (2012). Cooling of minichannel heat sink using nanofluids. *International Communications in Heat and Mass*, 39, 1188-1194.

Ijam, A. & Saidur, R. (2012). Nanofluid as a coolant for electronic devices. *Applied Thermal Engineering*, 32, 76-82.

Selvakumar, P. & Suresh, S. (2012). Convective performance of CuO/water nanofluid in an electronic heat sink. *Experimental Thermal and Fluid Science*, 40, 57-63.

Hashemi, S. M. H., Fazeli, S. A., & Zirakzadeh, H. (2012). Study of heat transfer enhancement in a nanofluid-cooled miniature heat sink. *International Communications in Heat and Mass*, 39, 877-884.

Khedkar, R. S., Sonawane, S. S., & Wasewar, K. L. (2013). Water to nanofluids heat transfer in concentric tube heat exchanger: Experimental study. *Procedia Enineering*, 51, 318-323.

Sun, B., Lei, W., & Yang, D. (2015). Flow and convective heat transfer characteristics of Fe_2O_3-water nanofluids inside copper tubes. *International Communications in Heat and Mass*, 64, 21-28.
Decagon Devices. (2010). *KD2 Pro Thermal Properties Analyzer Operator's Manual*, Washington: Pullman.